Enhanced Stability of Human Prion Proteins with Two Disulfide Bridges

Tuomas P. J. Knowles* and Ralph Zahn*†
*Institute of Molecular Biology & Biophysics, ETH Zurich, Zurich, Switzerland; and †alicon AG, Zürich-Schlieren, Switzerland

ABSTRACT We compare the folding equilibrium of the globular domain of the human prion protein with two variants of this domain, for which an additional disulfide bond was introduced into the location where it is found in the naturally occurring doppel protein. We find that the unfolding transition midpoint of the variants is shifted toward higher denaturant concentration, indicating that the engineered disulfide bond significantly stabilizes the global protein structure. Our results further reveal that the two-disulfide variant proteins, while possessing the same global fold as the wild-type, display marked differences in their folding pathway—in particular, the absence of a characteristic α-helix to β-sheet transition, which is a fundamental feature associated with misfolding of proteins into amyloid fibrils, especially in the context of prion diseases. These surprising characteristics of disulfide mutant prion proteins have important implications for the understanding of the generic aberrant processes leading to amyloid fibril formation and protein aggregation, as well as providing insight into possible therapeutic strategies.

INTRODUCTION

Prions are the infectious agents responsible for a group of fatal neurodegenerative diseases, including Creutzfeldt-Jakob disease in humans, which are characterized by the conversion of cellular prion protein (PrP^{C}) into the pathological scrapie form (PrP^{Sc}). Soluble recombinant prion proteins from various mammalian species have been shown to consist of two distinct domains: a 100-residue N-terminal tail of residues 23–120, which is flexibly disordered in large parts, and a well-structured C-terminal globular domain of residues 121–230 that is rich in α-helix secondary structure and contains a small antiparallel β-sheet and a single disulfide bond Cys^{179}–Cys^{214} (1–5). A two-disulfide variant hPrP (M166C/E221C) of this globular domain of the human prion protein hPrP (121–230) with an additional disulfide bond linking residues Cys^{166} and Cys^{221} has recently been prepared as a recombinant protein (6), where the design of the novel proteins was based on the location of the additional disulfide bond in the naturally occurring PrP-like Doppel protein (7) (Fig. 1 *b*). The nuclear magnetic resonance (NMR) structure of hPrP(M166C/E221C) (6) shows that this variant possesses the same global fold as wild-type hPrP(121–230) (Fig. 1), with the engineered additional disulfide bond being accommodated with slight, strictly localized conformational changes. High compatibility of hPrP structure with insertion of a second disulfide bridge between helix α_3 and the loop connecting helix α_2 and the second β-strand (Fig. 1) was further evidenced by expression and spectroscopic characterization of the variant protein hPrP(M166C/Y225C) and model calculations with additional variant structures (6).

Here, we have studied the pH dependence of guanidinium chloride (GdmCl) and temperature-induced unfolding of hPrP(M166C/E221C) and hPrP(M166C/Y225C) monitored with circular dichroism (CD) and compare the results to previously published structural and thermodynamic data of human and mouse prion proteins. Our measurements show that the variant proteins not only display a significantly enhanced stability but also marked differences in their folding pathway, in particular the absence of a β-sheet rich folding intermediate which is a characteristic of the mammalian prion proteins (8,9), and is thought to be involved in the pathological pathways leading to misfolding and aggregation of PrP^{Sc} in prion diseases.

METHODS

Protein production

The two variant proteins hPrP(M166C/E221C) and hPrP (M166C/Y225C) were expressed as inclusion bodies in *Escherichia coli* and purified by high-affinity column refolding (10), resulting in similar yield as for wild-type hPrP(121–230) (6). The formation of an additional disulfide bond was confirmed by mass spectrometry and NMR spectroscopy. The ^{1}H NMR spectra of both proteins showed that the preparations are homogeneous.

Spectroscopic characterization

Circular dichroism spectra were recorded with a JASCO J720 spectropolarimeter interfaced with a Peltier-type temperature control unit, with 1 mm or 0.2 mm pathlength cuvette. The ellipticity at 222 nm was used for monitoring GdmCl-induced unfolding. Measurements were performed at pH 7 in buffer containing 20 mM sodium phosphate and at pH 5 in buffer containing 20 mM sodium acetate.

Congo Red spectroscopic assay

A solution of Congo Red was freshly dissolved at 7 mg/mL in PBS buffer (5 mM potassium phosphate, 150 mM NaCl, pH 7.4) and filtered through a 0.2-μm syringe filter. Absorptions spectra were recorded using a Tecan Safire Multi-Detection Monochrometer Microplate Reader (Tecan, Stäfa, Switzerland)

Submitted January 19, 2006, and accepted for publication May 22, 2006.

Address reprint requests to R. Zahn, Fax: 41-43-495-05-69; E-mail: info@alicon.ch.

Tuomas P. J. Knowles's present address is Cavendish Laboratory, Dept. of Physics, and Nanoscience Centre, Dept. of Engineering, University of Cambridge, J. J. Thomson Ave., Cambridge CB3 0HE, UK.

0006-3495/06/08/1494/07 $2.00

doi: 10.1529/biophysj.106.081653

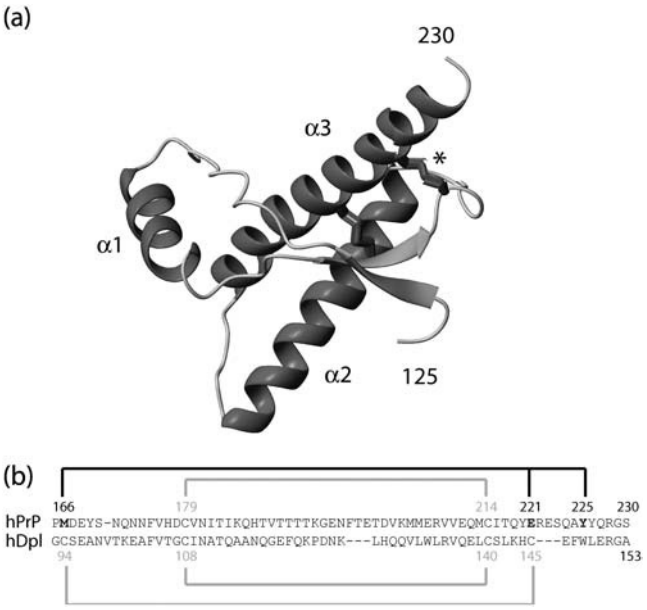

FIGURE 1 (*a*) Ribbon-drawing of the three-dimensional structure of hPrP(M166C/E221C) (6). The engineered additional disulfide bond Cys-166–Cys-221 is indicated with an asterisk. The figure was prepared with the program MOLMOL (31). In panel *b*, sequence alignment of the human prion protein segment 165–230 and the human doppel protein segment 93–153, showing the natural disulfide bonds (*shaded lines*) and location of the additional disulfide bond (*solid line*) for the hPrP(M166C/Y225C) and (M166C-E221C) mutants, which is inspired from the corresponding location in the naturally occurring doppel. The residues which were changed are in bold.

between 400 and 700 nm at room temperature using volumes of 200 μl. First the spectrometer was zeroed using only the buffer solution. Then 1 μl of the Congo Red stock solution was added to 199 μl of the buffer and the spectrum recorded to serve as a control. Solutions of the prion proteins were prepared at a concentration of 1 mg/ml in buffer containing 20 mM sodium phosphate at pH 7 and in buffer containing 20 mM sodium acetate and 1 M GdnHCl at pH 5. Subsequently 20 μl of the protein solution was added to 179 μl of PBS buffer and 1 μl of Congo Red solution, and the spectrum was measured after 10 min of incubation. Additionally, as a positive control, hPrPβ(23–230)(Alicon PrP-beta, Alicon, Schlieren, Switzerland) was used.

Mathematical modeling and fitting

Denaturation curves were fitted to a two-state model, assuming that the free energy ΔG of unfolding is linearly dependent upon the concentration of denaturant [D] present in the solution (11,12): $\Delta G = \Delta G^0 + m[\mathrm{D}]$, where m is the cooperativity of unfolding and ΔG^0 is ΔG in the absence of denaturant. Evaluation of the equilibrium constants in the transition region was obtained by extrapolation of the pre- and post-transitional baselines into the transition region. The two-state model used to fit the data assumes the dependence of the observed signal, S_{obs}, as

$$S_{\mathrm{obs}} = \frac{(S_{\mathrm{N}}^0 + m_{\mathrm{N}}[\mathrm{D}])\exp\left(-\dfrac{\Delta \mathrm{G}^0 + \mathrm{m}[\mathrm{D}]}{\mathrm{RT}}\right) + S_{\mathrm{D}}^0 + m_{\mathrm{D}}[\mathrm{D}]}{1 + \exp\left(-\dfrac{\Delta \mathrm{G}^0 + \mathrm{m}[\mathrm{D}]}{\mathrm{RT}}\right)},$$

where S_{N}^0 and S_{D}^0 are the intercepts; m_{N} and m_{D} are the slopes of the pre- and post-transition regimes, respectively; T is the absolute temperature in Kelvin; and R is the ideal gas constant. In particular, the transition midpoint $[\mathrm{D}]_{1/2}$ can be determined from the condition that the argument in the exponentials vanishes, yielding $[\mathrm{D}]_{1/2} = \Delta G^0/m$.

Thermally induced unfolding

Protein concentration was 24 μM in 10 mM sodium acetate at pH 4.5. Thermal denaturation experiments were performed by monitoring the circular dichroism at 222 nm, while changing the temperature from 10°C to 90°C with a constant rate of change of 50°C per hour. The unfolding experiments were performed twice, and very similar results were obtained.

RESULTS

Stabilization of globular protein structure

The globular protein stability of wild-type hPrP(121–230) and the variant proteins were measured by monitoring the molar ellipticity at 222 nm in solutions containing different concentrations of GdmCl. At pH 7.0, hPrP(121–230) undergoes a highly cooperative two-state transition (Fig. 2 *a*) with a midpoint of transition $[\mathrm{D}]_{1/2} = 2.1$ M and a free energy of unfolding in the absence of denaturant $\Delta G_0 = -19$ kJ mol^{-1}. These thermodynamic values are nearly identical

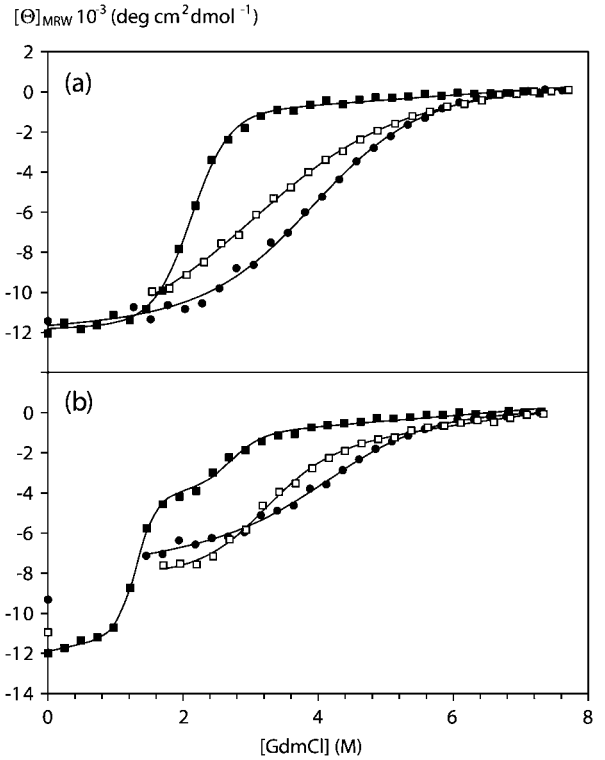

FIGURE 2 GdmCl-dependent mean residue molar ellipticity of human prion proteins. (*a*) In buffer containing 20 mM sodium phosphate at pH 7.0. (*b*) In buffer containing 20 mM sodium acetate at pH 5.0. The spectra in panels *a* and *b* were recorded with 30 μM protein solutions at 22°C: solid squares, wild-type hPrP(121–230); open squares, hPrP(M166C/Y225C); and solid circles, hPrP(M166C/E221C).

to those determined for the prion protein construct hPrP(90–231) (8). A single folding transition was also observed for the two hPrP(121–230) disulfide variant proteins (Fig. 2 *a*). However, hPrP(M166C/E221C) and hPrP(M166C/Y225C) showed an increase in the transition midpoint $[D]_{1/2}$, indicating that the global structures are stabilized by the engineered disulfide bonds (13,14). The lower folding cooperativity of the variant proteins indicates a deviation from a two-state folding mechanism.

Absence of β-sheet rich folding intermediate in the folding pathway of disulfide mutant prions

At pH 5.0, wild-type hPrP(121–230) shows two distinctive folding transition regions with transition midpoints at 1.3 and 2.7 M GdmCl, clearly indicating the presence of a folding intermediate that is maximally populated at ~2 M GdmCl (Fig. 2 *b*). The existence of a stable folding intermediate during equilibrium unfolding in GdmCl has also been reported for hPrP(90–231) (8).

Although the two cysteine variant proteins are soluble up to 1 mM protein concentration in the absence of denaturant, their decreased solubility at low GdmCl concentration precluded quantitative CD measurements (Fig. 2 *b*) so that we were not able to determine the folding transition model for these proteins. Similar to the data obtained at neutral pH, the observed folding transition midpoints of hPrP(M166C/E221C) and hPrP(M166C/Y225C) are shifted toward higher molarities of denaturant with respect to the second transition midpoint of hPrP(121–230), and the folding cooperativity is decreased (Fig. 2 *b*).

To gain insight into the conformational properties of the human prion proteins under conditions corresponding to the presence of the stable folding intermediate of wild-type hPrP(121–230), we measured far-UV CD spectra at pH 5.0 in the presence and absence of 2 M GdmCl. The spectra of the three proteins in the absence of denaturant are essentially similar (Fig. 3), with the minima at 208 and 222 nm indicating a largely α-helical structure (5,6). The slight differences in the spectra of the variant proteins relative to the wild-type can be understood as a consequence of the additional absorption from the second disulfide-bond in the far-UV region (15), since the structures are very similar apart from small localized changes around the disulfide bridge insertion points (6). Furthermore, it is known from NMR chemical shift measurements that the population of α-helical secondary structure within helix α3 of both hPrP(M166C/E221C) and hPrP(M166C/Y225C) is slightly decreased (6).

At 2 M GdmCl, where the folding intermediate of wild-type hPrP(121–230) is maximally populated, the double minimum in the CD spectrum of hPrP(121–230) is replaced by a single minimum at 213 nm (Fig. 3 *a*), which is characteristic of proteins rich in β-sheet secondary structure. A similar monomeric folding intermediate has been described at pH 4.0 for hPrP(90–231), which is maximally populated at 1 M GdmCl (8), and also for mouse PrP(121–231) at 4 M urea (9). It has been postulated that these intermediates—which remarkably are absent in our disulfide variant proteins as discussed below—may represent a soluble precursor of PrP^{Sc}. Such models are consistent with the current understanding of the generic events associated with amyloid fibril formation, which involve partially unfolded structures that first reversibly form prefibrillar β-sheet rich species and then finally assemble to form the mature amyloid fibrils (16). Recent

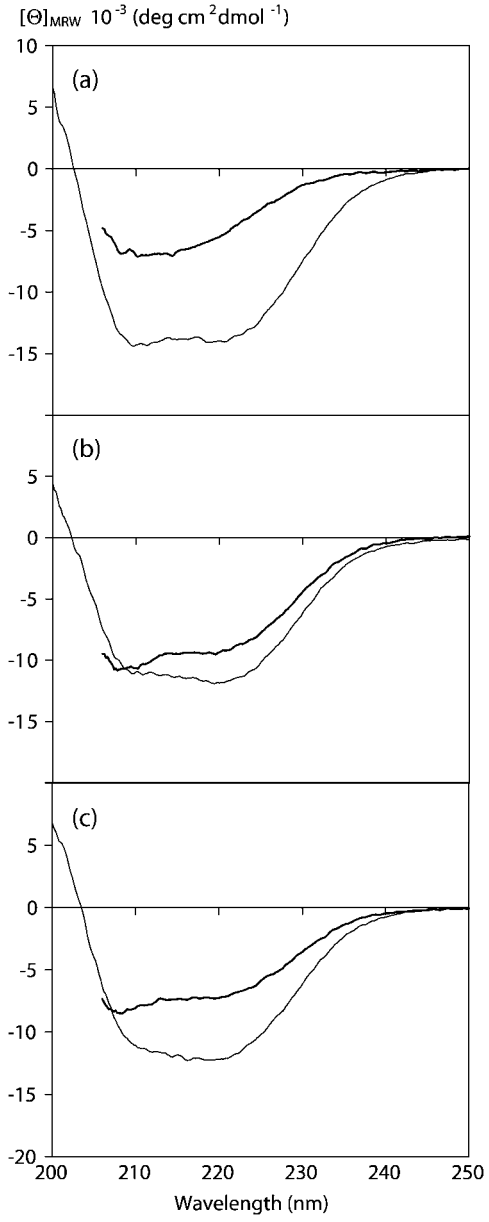

FIGURE 3 Circular dichroism spectra of human prion proteins. (*a*) Wild-type hPrP(121–230); (*b*) hPrP(M166C/E221C); and (*c*) hPrP(M166C/Y225C). The spectra were recorded with 20 μM protein solutions in 20 mM sodium acetate at pH 5.0 and 22°C, either in the presence (*bold line*) or in the absence (*thin line*) of 2 M GdmCl.

evidence (17) suggests, however, that multiple pathways exist for the misfolding of hPrP(91–231) (17), and only some intermediates are likely to be involved in vivo in the processes that, starting from normal soluble prion proteins, produce pathological aggregates, thus explaining the complexity of producing infectious prions in vitro.

On the other hand, the CD spectra of the two variant prion proteins in 2 M GdmCl remain typical for a protein rich in α-helix structure (Fig. 3, *b* and *c*), indicating that there is no accumulation of a folding intermediate with increased β-sheet structure. The relative increase in amplitude at 208 nm versus 222 nm, when compared with the native protein, may be rationalized by a partial transition of α-helix into a random coil conformation, but there is no evidence for an α-helix-to-β-sheet transition in the presence of GdmCl, as is the case for wild-type protein. Thus, the introduction of a second disulfide bond into the globular prion protein domain not only results in increased overall protein stability, but also introduces novel features into folding pathways of the proteins, which otherwise have the same native fold.

Finally, inspired by the elegant experiments of Baskskov et al. (17) and considering that the disulfide mutant proteins showed evidence of reduced solubility in the region corresponding to 0 M $<$ [GdmCl] $<$ 2 M, we examined by using Congo Red binding assays whether there were signs of amyloid fibril formation under these conditions. This is especially relevant at pH 5, where the wild-type protein is folding into the intermediate maximally populated at 2 M GdmCl, which has a predominantly β-sheet character, a feature which appears to be shared among many mammalian prions constructs (8,9), and places the confirmation closer structurally to that acquired in amyloid fibrils. The absorbance spectrum of Congo Red displays a characteristic red-shift when the dye is bound to amyloid (18); which specific effect is thought to be due to the interaction of the planar molecule with the cross-β core structure in amyloid fibrils. We found, as shown in Fig. 4, that the absorption spectrum of both mutants under these conditions did not show any significant shift, suggesting that any aggregation in this regime is of an amorphous nature and not composed of amyloid fibrils. On the other hand, suspended aggregates of amyloid fibrils that formed from hPrPβ(23–230) (19) under these conditions display the characteristic red-shift in the absorption, which spectroscopically confirms their fibrillar nature (Fig. 4).

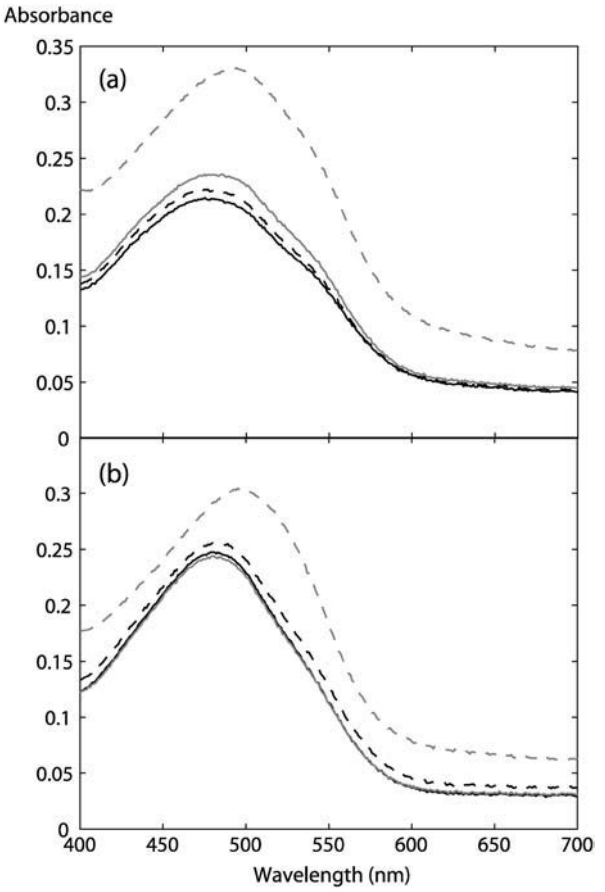

FIGURE 4 Congo Red binding assays of human prion proteins. Absorptions spectrum (*a*) at pH 5 in 1M GdmCl for hPrP(M166C/E221C) (*black dashed line*), hPrP(M166C/Y225C) (*solid line*), hPrP(121–230) (*shaded line*), and hPrPβ(23–230) (*shaded dashed line*). Only hPrPβ(23–230) shows the characteristic red-shift of the absorptions maxima from 480 nm to 500 nm and the development of a shoulder at 540 nm (18), which indicate the presence of amyloid fibrils. For comparison (*b*), in data at pH 7 0M GdmCl is shown, where similar observations hold.

Increase in thermal stability of the protein structure

To refine our understanding of the fundamental differences in the folding of the disulfide mutant prion proteins, the effects of elevated temperature were investigated. The thermal unfolding of the three prion proteins under acidic conditions occurs in a single transition (Fig. 5), but, as for GdmCl-induced unfolding previously discussed, the qualitatively different equilibrium unfolding characteristics of wild-type versus variant proteins induced is also manifested. The two-state thermal unfolding of hPrP(121–230) is highly cooperative with a melting temperature of ~60°C (Fig. 5 *a*). The folding transition of hPrP(M166C/Y225C) and hPrP(M166C/E221C) is much less cooperative, and is shifted by $>$10°C toward higher temperatures (Fig. 5, *b* and *c*), reflecting again the greater stability. The exact temperature of the folding transition could not be determined for the variant proteins, because even at 100°C they have not reached the post-unfolding regime and contain a significant degree of protein secondary structure with negative ellipticity at 222 nm.

DISCUSSION

A generic feature of prion diseases is the misfolding of soluble prion protein into amyloid fibrils and other higher order aggregates. This process is likely to be the key to

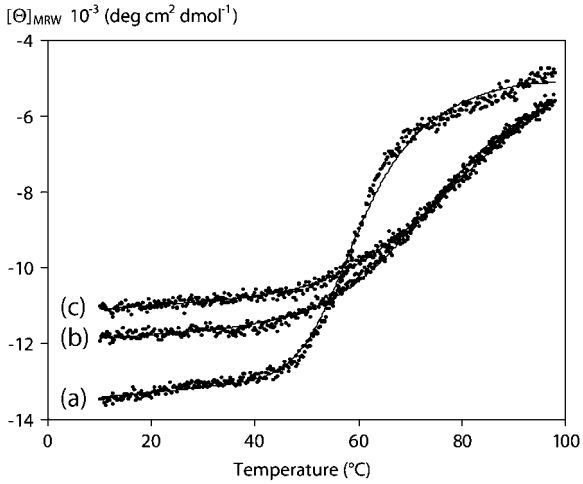

FIGURE 5 Temperature-dependent mean residue molar ellipticity of human prion proteins. (*a*) Wild-type hPrP(121–230); (*b*) hPrP(M166C/Y225C); and (*c*) hPrP(M166C/E221C).

understanding both the evolution and the transmissibility of such disease states, which implies that the characterization of the folding pathways of prion proteins is essential for developing models of, and eventually therapies against, these pathogenic events (17).

We introduced an additional disulfide bond into the globular domain of the prion protein at the analog location where it is found in the doppel protein (20), which has two disulfide bridges (Fig. 1 *b*), and found that this influenced dramatically the folding pathway of the protein, despite leaving the native structure of the protein nearly untouched. The stability of the native state was greatly enhanced, and the characteristic α-to-β transition was removed from the folding pathway. It is interesting to compare these results with the equivalent measurements for the doppel protein: Whyte et al. (20) studied both the wild-type doppel protein and a certain mutant where the disulfide bridge, corresponding to the location where it is found in the prion proteins, was kept but the second one was removed—exactly the complement of this work. It was found that removing the disulfide bond destabilized the native structure of the doppel protein, in agreement with our present conclusion that making the prion protein more doppel-like increased its stability. However, it was found that even for the prionlike doppel protein with only one disulfide bond, the unfolding was a two-state process, with no evidence of the α-to-β transition characteristic of the prion proteins. This implies that the presence of this intermediate in the unfolding process of prion proteins depends on the sequence differences between the doppel and the prion proteins and even though our doppel-like prion proteins lose this feature, it cannot be restored in prionlike doppel proteins by the simple deletion of the corresponding disulfide bond (20).

We finally wish to discuss some implications for ideas with regard to therapeutic aspects. Currently there are no drugs available for the treatment of prion diseases in humans and animals (21,22). Within the framework of the protein-only hypothesis (23), at least two mechanisms can be imagined that could prevent the accumulation of toxic misfolded protein conformations resulting in TSE. The first mechanism relies on a PrP^C-binder that specifically binds to the normal form of the prion protein, thus preventing PrP^C from folding into PrP^{Sc}. The second mechanism would use a PrP^{Sc}-binder to either block the homophilic assembly of PrP^{Sc} into amyloid fibrils or to interfere with a heterophilic interaction with other macromolecules that otherwise are implicated in pathogenic pathways. The advantage of PrP^{Sc}-binders over PrP^C-binders is that they do not interfere with the yet unknown physiological function of the cellular form of the protein. Only a few compounds with therapeutic potential, including a monoclonal PrP^{Sc}-binding antibody (24) and a 13-residue β-sheet breaker peptide (25), have been identified which specifically bind to the scrapie conformation of prion proteins. Another strategy in this direction that has been suggested for TSE treatment is based on the design of soluble PrP derivatives that bind to PrP^{Sc}, but cannot be converted by a template-assisted mechanism and thus inactivate the bound PrP^{Sc} molecule. Bürkle and co-workers have shown that the presence of amino acids 114–121 of mouse PrP plays an important role in the conversion of PrP^C into PrP^{Sc} and that a deletion mutant lacking these residues behaves as a dominant negative mutant with respect to PrP^{Sc} accumulation in cell culture (26). Recently, Aguzzi and co-workers constructed a soluble dimeric prion protein that binds PrP^{Sc} in vivo and antagonizes prion disease (27). Dominant negative inhibition could thus form a basis for treatment or prevention of prion diseases.

The combination of earlier structural data (6) and the present thermodynamical data on hPrP(M166C/E221C) and hPrP(M166C/Y225C) suggests that disulfide variants of PrP may also be applicable as a dominant negative treatment for prion diseases. Clearly, the data presented in this work show that these novel proteins stabilized by an additional disulfide bond are either denatured or in a PrP^C-like conformation. This feature makes them good candidates as inhibitors of PrP^{Sc} formation assuming a heteroduplex-model for PrP conversion (28), i.e., a model involving a transient complex between PrP^C and PrP^{Sc}. In fact, recombinant two-disulfide PrP^C might be used to demonstrate the existence of a heterodimeric complex with native PrP^{Sc}. The preservation of the native three-dimensional structure in the PrP variants (6) makes it likely that these have a similar affinity to PrP^{Sc} as does wild-type PrP^C. The PrP^{Sc}-binding site of PrP^C is not known, but there is evidence from genetic experiments (29, 30) that the region of helix α1 (residues 144–154 in human PrP) and the preceding loop region (residues 132–143 in human PrP) are involved in PrP^{Sc} binding. This region is structurally unchanged after introduction of an additional disulfide bond between helix α3 and the loop connecting helix α2 and the second β-strand (6). The increased

$[D]_{1/2}$-values in Fig. 2 and melting temperatures in Fig. 4 of the variant proteins indicate that a higher amount of free energy is required for transforming PrP^{Sc}-bound two-disulfide PrP^{C} into a conformation that is competent for folding into PrP^{Sc}. Therefore, the additional disulfide bonds in the variant proteins should, per se, decrease efficiency of prion propagation and thus delay progression of prion disease. At acidic pH, the protection against a conversion into a pathogenic protein conformation presumably may be even more pronounced, because the α-helix secondary structure of the variant proteins resists a conformational transition into β-sheet secondary structure, as shown in Fig. 3, *b* and *c*. Thus, within the environment of endosomes or lysosomes, PrP^{Sc} would probably become trapped in an inactive complex with a bound PrP^{C} disulfide variant that is unable to promote prion propagation.

It will be of interest to investigate if such a mechanism of blocking the growth of PrP^{Sc} fibrils by forming a stable heterodimeric complex can be established during future cell culture and animal experiments, where the recombinant disulfide variant prion proteins could be intraperitoneally inoculated or may be even expressed in vivo using a gene therapeutic approach.

In conclusion, we have shown how, without modifying the native fold of the human prion protein, it is possible to significantly enhance its structural stability, and change the folding pathway such that potentially amyloidogenic intermediates are not present. These findings shed light on possible general therapeutic concepts and strategies for the treatment of a variety of neurodegenerative diseases.

We are grateful to Christine von Schroetter for preparation of recombinant prion proteins and to Glyn Devlin for insightful discussions and advice on the Congo Red binding assays. We also thank Patrik Buchholzer and Prionics AG for assistance with the absorption spectroscopy, Fred Damberger for critically reading the manuscript, and Kurt Wüthrich for helpful discussions.

REFERENCES

1. Riek, R., S. Hornemann, G. Wider, M. Billeter, R. Glockshuber, and K. Wüthrich. 1996. NMR structure of the mouse prion protein domain PrP(121–321). *Nature*. 382:180–182.
2. Liu, H., S. Farr-Jones, N. B. Ulyanov, M. Llinas, S. Marqusee, D. Groth, F. E. Cohen, S. B. Prusiner, and T. L. James. 1999. Solution structure of Syrian hamster prion protein rPrP(90–231). *Biochemistry*. 38:5362–5377.
3. James, T. L., H. Liu, N. B. Ulyanov, S. Farr-Jones, H. Zhang, D. G. Donne, K. Kaneko, D. Groth, I. Mehlhorn, S. B. Prusiner, and F. E. Cohen. 1997. Solution structure of a 142-residue recombinant prion protein corresponding to the infectious fragment of the scrapie isoform. *Proc. Natl. Acad. Sci. USA*. 94:10086–10091.
4. Garcia, F. L., R. Zahn, R. Riek, and K. Wüthrich. 2000. NMR structure of the bovine prion protein. *Proc. Natl. Acad. Sci. USA*. 97: 8334–8339.
5. Zahn, R., A. Liu, T. Lührs, R. Riek, C. von Schroetter, F. L. Garca, M. Billeter, L. Calzolai, G. Wider, and K. Wüthrich. 2000. NMR solution structure of the human prion protein. *Proc. Natl. Acad. Sci. USA*. 97:145–150.
6. Zahn, R., P. Güntert, C. von Schroetter, and K. Wüthrich. 2003. NMR structure of a variant human prion protein with two disulfide bridges. *J. Mol. Biol.* 326:225–234.
7. Mo, H., R. C. Moore, F. E. Cohen, D. Westaway, S. B. Prusiner, P. E. Wright, and H. J. Dyson. 2001. Two different neurodegenerative diseases caused by proteins with similar structures. *Proc. Natl. Acad. Sci. USA*. 98:2352–2357.
8. Swietnicki, W., R. Petersen, P. Gambetti, and W. K. Surewicz. 1997. pH-dependent stability and conformation of the recombinant human prion protein PrP(90–231). *J. Biol. Chem.* 272:27517–27520.
9. Hornemann, S., and R. Glockshuber. 1998. A scrapie-like unfolding intermediate of the prion protein domain PrP(121–231) induced by acidic pH. *Proc. Natl. Acad. Sci. USA*. 95:6010–6014.
10. Zahn, R., C. von Schroetter, and K. Wüthrich. 1997. Human prion proteins expressed in *Escherichia coli* and purified by high-affinity column refolding. *FEBS Lett*. 417:400–404.
11. Santoro, M. M., and D. W. Bolen. 1988. Unfolding free energy changes determined by the linear extrapolation method. 1. Unfolding of phenylmethanesulfonyl α-chymotrypsin using different denaturants. *Biochemistry*. 27:8063–8068.
12. Bolen, D. W., and M. M. Santoro. 1988. Unfolding free energy changes determined by the linear extrapolation method. 2. Incorporation of δG° *N-U* values in a thermodynamic cycle. *Biochemistry*. 27:8069–8074.
13. Fersht, A. R. 1993. The sixth Datta Lecture. Protein folding and stability: the pathway of folding of barnase. *FEBS Lett*. 325:5–16.
14. Fersht, A. R. 1994. Jubilee Lecture. Pathway and stability of protein folding. *Biochem. Soc. Trans*. 22:267–273.
15. Coleman, D. L., and E. R. Blout. 1968. The optical activity of the disulfide bond in L-cysteine and some derivatives of L-cysteine. *J. Am. Chem. Soc*. 90:2405–2416.
16. Dobson, C. M. 2003. Protein folding and misfolding. *Nature*. 426: 884–890.
17. Baskakov, I. V., G. Legname, M. A. Baldwin, S. B. Prusiner, and F. E. Cohen. 2002. Pathway complexity of prion protein assembly into amyloid. *J. Biol. Chem*. 277:21140–21148.
18. Nilsson, M. R. 2004. Techniques to study amyloid fibril formation in vitro. *Methods*. 34:151–160.
19. Lührs, T., R. Zahn, and K. Wüthrich. 2006. Amyloid formation by recombinant full-length prion proteins in phospholipid bicelle solutions. *J. Mol. Biol*. 357:833–841.
20. Whyte, S. M., I. D. Sylvester, S. R. Martin, A. C. Gill, F. Wopfner, H. M. Schatzl, G. G. Dodson, and P. M. Bayley. 2003. Stability and conformational properties of doppel, a prion-like protein, and its single disulphide mutant. *Biochem. J*. 373:485–494.
21. Follette, P. 2003. New perspectives for prion therapeutics meeting. Prion disease treatment's early promise unravels. *Science*. 299:191–192.
22. Hill, A. F., and J. Collinge. 2003. Subclinical prion infection. *Trends Microbiol*. 11:578–584.
23. Prusiner, S. B. 1998. Prions. *Proc. Natl. Acad. Sci. USA*. 95:13363–13383.
24. Korth, C., B. Stierli, P. Streit, M. Moser, O. Schaller, R. Fischer, W. Schulz-Schaeffer, H. Kretzschmar, A. Raeber, U. Braun, F. Ehrensperger, S. Hornemann, R. Glockshuber, R. Riek, M. Billeter, K. Wuthrich, and B. Oesch. 1997. Prion (PrPSc)-specific epitope defined by a monoclonal antibody. *Nature*. 390:74–77.
25. Soto, C., R. J. Kascsak, G. P. Saboro, P. Aucouturier, T. Wisniewski, F. Prelli, R. Kascsak, E. Mendez, D. A. Harris, J. Ironside, F. Tagliavini, R. I. Carp, and B. Frangione. 2000. Reversion of prion protein conformational changes by synthetic β-sheet breaker peptides. *Lancet*. 355:192–197.
26. Hölscher, C., H. Delius, and A. Bürkle. 1998. Overexpression of nonconvertible PrPc δ114–121 in scrapie-infected mouse neuroblastoma cells leads to trans-dominant inhibition of wild-type PrP(Sc) accumulation. *J. Virol*. 72:1153–1159.

27. Meier, P., N. Genoud, M. Prinz, M. Maissen, T. Rlicke, A. Zurbriggen, A. J. Raeber, and A. Aguzzi. 2003. Soluble dimeric prion protein binds PrP(Sc) in vivo and antagonizes prion disease. *Cell.* 113:49–60.

28. Prusiner, S. B., M. Scott, D. Foster, K. M. Pan, D. Groth, C. Mirenda, M. Torchia, S. L. Yang, D. Serban, and G. A. Carlson. 1990. Transgenetic studies implicate interactions between homologous PrP isoforms in scrapie prion replication. *Cell.* 63:673–686.

29. Telling, G. C., M. Scott, K. K. Hsiao, D. Foster, S. L. Yang, M. Torchia, K. C. Sidle, J. Collinge, S. J. DeArmond, and S. B. Prusiner. 1994. Transmission of Creutzfeldt-Jakob disease from humans to transgenic mice expressing chimeric human-mouse prion protein. *Proc. Natl. Acad. Sci. USA.* 91:9936–9940.

30. Telling, G. C., M. Scott, J. Mastrianni, R. Gabizon, M. Torchia, F. E. Cohen, S. J. DeArmond, and S. B. Prusiner. 1995. Prion propagation in mice expressing human and chimeric PrP transgenes implicates the interaction of cellular PrP with another protein. *Cell.* 83:79–90.

31. Koradi, R., M. Billeter, and K. Wüthrich. 1996. MOLMOL: a program for display and analysis of macromolecular structures. *J. Mol. Graph.* 14:51–55.